engineering proceedings

MDPI

Proceeding Paper

Low-Cost Remote Sensing Module for Agriculture 4.0 Based on STM32 †

Gustavo Gimenes [1], Wenderson Nascimento Lopes [1,*], Ronald José Contijo [1], Reinaldo Götz de Oliveira Junior [2] and Renan de Oliveira Alves Takeuchi [1]

[1] Department of Industrial Control and Processes, Paraná Federal Institute of Education (IFPR), Jacarezinho 86400-000, Paraná, Brazil; ggimenes114@gmail.com (G.G.); ronaldcontijofunciona@gmail.com (R.J.C.); renan.takeuchi@ifpr.edu.br (R.d.O.A.T.)
[2] Department of Industrial Control and Processes, Mato Grosso do Sul Federal Institute of Education (IFMS), Três Lagoas 79641-162, Mato Grosso do Sul, Brazil; reinaldo.oliveira@ifms.edu.br
* Correspondence: wenderson.lopes@ifpr.edu.br
† Presented at the 12th International Electronic Conference on Sensors and Applications, 12–14 November 2025; Available online: https://sciforum.net/event/ECSA-12.

Abstract

Agriculture 4.0 integrates smart technologies to optimize agricultural management. This work proposes the development of a low-cost remote sensing module for small producers in the north of Paraná, Brazil, using the STM32F411CEU6 (STMicroelectronics, Geneva, Switzerland) microcontroller and the nRF24L01 (Nordic Semiconductor, Trondheim, Norway) + module for mesh communication. The system measures temperature, humidity, and pressure using DS18B20, BME280, and capacitive soil moisture sensors via Inter-Integrated Circuit (I^2C), Serial Peripheral Interface (SPI), and Analog-to-Digital Converter (ADC). Powered by a solar cell and Lithium Polymer (Li-Po) battery, along with a charge controller, the module acts as a transceiver, sending data to a gateway where it can be stored and analyzed, democratizing access to technology and supporting decision-making in crop management.

Keywords: embedded systems; agronomy; microcontrollers

check for updates

Academic Editor: Stefano Mariani

Published: 7 November 2025

Citation: Gimenes, G.; Lopes, W.N.; Contijo, R.J.; de Oliveira Junior, R.G.; de Oliveira Alves Takeuchi, R. Low-Cost Remote Sensing Module for Agriculture 4.0 Based on STM32. *Eng. Proc.* **2025**, *118*, 97. https://doi.org/10.3390/ECSA-12-26544

Copyright: © 2025 by the authors. Licensee MDPI, Basel, Switzerland. This article is an open access article distributed under the terms and conditions of the Creative Commons Attribution (CC BY) license (https://creativecommons.org/licenses/by/4.0/).

1. Introduction

The climate crisis has become an increasing challenge for agriculture. According to Cerri [1], "until recently, farmers relied exclusively on well-established and extensively studied techniques, adjusted to the climatic patterns historically expected for certain times of the year. However, the recent climatic unpredictability has drastically altered these scenarios and compromised crops" [1].

In this context, technology emerges as an essential ally to face the challenges imposed by climate change, integrating into the agricultural sector with the goal of improving productivity without the need to expand cultivated land.

According to researcher Regis [2], in a study conducted at the University of Brasília (UnB), the digitalization of agriculture in Brazil has increasingly attracted the attention of producers, consolidating itself as an irreversible process. This technological transformation contributes to greater productive efficiency and added value in agricultural products, in addition to enabling more effective soil management.

However, this reality is not yet accessible to all. Small and medium-sized producers face difficulties, either due to the high cost of implementing these technologies or the lack

of information about their benefits and applications. In many cases, these farmers restrict the use of digital tools to basic activities, such as banking transactions or checking weather forecasts, without fully exploring their potential in managing the production system [2].

Precision agriculture, originating from the third agricultural revolution, proposes an integrated approach to agribusiness management. By employing agricultural machinery integrated with electronic technologies, this practice aims to increase production efficiency and soil profitability. Its main distinguishing feature lies in the intensive collection and analysis of data, enabling evidence-based strategic decision-making.

Soil monitoring is one of the tools of precision agriculture and aims to collect as much information as possible throughout all stages of cultivation, especially data on the physical and chemical aspects of the soil and the atmosphere. Mini weather stations are devices equipped with sensors capable of monitoring a wide range of climatic variables. Powered by photovoltaic cells, they can operate in fields and plantations located far from the electrical grid.

There are several examples of such equipment available on the market, such as the S-THB-M003 wireless agricultural monitoring sensor, developed by Milesight, which costs around USD 180.00 per module, in addition to implementation and importation fees. This represents a high investment cost for small and medium-sized rural producers, who in Brazil have been receiving increasingly smaller investments compared to those directed at large producers. In 2024, BRL 189 billion was allocated to the National Support Program for Medium-Sized Rural Producers (Pronamp), and only BRL 14.8 billion to the National Program for Strengthening Family Farming (Pronaf)—a relatively small amount compared to the BRL 400 billion invested in large producers [3].

Some of the primary impacts of precision agriculture are related to both economic and environmental aspects. From a financial perspective, the adoption of this technology enables the generation of a robust and detailed database that supports strategic analyses. In this way, producers can make more assertive decisions regarding water consumption, the use of agricultural inputs—such as fertilizers and pesticides—and the adoption of preventive measures, resulting in significant cost reductions without compromising crop productivity [4].

From an environmental perspective, the accuracy in the application of inputs directly contributes to soil conservation and the protection of agricultural ecosystems. In addition to reduced water consumption, a key practice is the localized application of fertilizers and pesticides, restricted only to areas that actually require them, thereby minimizing negative environmental impacts [5].

A survey of the state of the art in related works was conducted with the aim of establishing comparisons with similar systems. Some of the articles that showed the greatest similarity with the addressed topic were [6,7], both related to the development of agricultural sensing modules. It was observed that most proposed solutions employ microcontrollers such as ESP32, Arduino, and Raspberry Pi, generally associated with Wi-Fi communication at all data collection points. However, a gap was identified regarding the use of STM32 microcontrollers, which remain scarcely explored in this context. This finding reinforces the relevance of directing the present work towards the use of STM32, thereby expanding the scope of existing solutions and contributing to technological diversification in the field. Furthermore, the integration of STM32 with radio frequency modules enables access to regions lacking Wi-Fi coverage, which are predominant in rural environments.

Thus, this article proposes the development of a low-cost embedded module using the STM32 microcontroller, with an estimated value of up to R$350.00, capable of providing real-time information on essential parameters for agricultural management, such as soil temperature and moisture, as well as atmospheric humidity, pressure, and temperature. The

goal is to expand access for small and medium-sized farmers to environmental monitoring technologies without the need for large investments, allowing them to accurately track their crop conditions. For user interaction, a web interface for module management, visualization of the collected data, and provision of specific insights is being developed concurrently with this work. However, its description lies beyond the scope of this article. In this way, the aim is to support more accurate decision-making, optimize resource allocation, and contribute to increased productivity and harvest efficiency.

2. Component Selection

The STM32 microcontrollers, produced by STMicroelectronics, are known for their versatility, with models ranging from high-performance (STM32F4 series) to ultra-low-power (STM32L0 series) devices [8]. They do not include integrated wireless modules such as Wi-Fi or Bluetooth but offer a wide variety of peripherals, memory sizes, and performance levels that make them suitable for a broad range of applications.

STM32 devices based on the HAL (Hardware Abstraction Layer) library are highly versatile, as they require drivers for interfacing with external modules, allowing full control of hardware configurations through direct register access. In terms of power efficiency, the STM32F411CEU6—running at a CPU clock speed of 80 MHz—typically consumes about 8 mA in run mode [9]. Additionally, the STM32CubeIDE, the official integrated development environment provided by STMicroelectronics, offers precise visual configuration of communication protocols, pin assignments, and clock frequencies.

For prototyping, the STM32F411CEU6, commercially available on the BlackPill development board, stands out as an excellent choice due to its balance between versatility, performance, and low power consumption.

Two radio frequency transmission modules stand out: the E220–400T from EBYTE and the nRF24L01+ from Nordic Semiconductor. Both use LNA technology for noise reduction and PA for signal amplification, operating via SPI protocol. The E220 supports larger packets (200 bytes) and transmission power up to 22 dBm, reaching up to 10 km [10], while the nRF24L01 transmits packets up to 32 bytes with 0 dBm power and a range of 1 km under ideal conditions.

The nRF24L01+ consumes less energy (11.3 mA at max power) compared to the E220–400T's peak of 110 mA and offers higher data rates (2 MB/s vs. 62.5 KB/s). Its key advantage lies in its architecture: five independent data channels, dynamic payload length, and the Enhanced Shock Burst (ESB) protocol, which automatically retransmits packets without microcontroller intervention [11]. The module also features an IRQ pin for critical event signaling, enabling quick interruption handling to ensure no packets are lost. Due to the benefits of automatic message retransmission provided by the Enhanced ShockBurst protocol and its low power consumption, the nRF24L01+ PA/LNA was selected for the prototype. To overcome the limitation of short transmission range, a software-based solution is being developed. This approach relies on message retransmission across the network, where each module functions as a routing node, thereby enabling coverage of longer distances.

In atmospheric sensing, some variables are essential for monitoring, such as temperature, humidity, and pressure. Sensors like the HTS221 [12], SHT31 [13], and SHTC3 [14] (both from Sensirion) only monitor temperature and humidity, excluding pressure. Conversely, sensors like the BMP280 [15] and LPS22HB [16] measure only temperature and atmospheric pressure. Despite their ultra-low power consumption and compact size, none of these sensors can measure all three atmospheric variables on the same chip.

However, Bosch's BME280 sensor (not to be confused with the BMP280) offers simultaneous measurement of pressure, humidity, and temperature. It supports dynamic

configurations and can operate via I2C or SPI communication protocols. It also includes an IIR (Infinite Impulse Response) filter to smooth readings and reduce fluctuations. Additionally, its operating modes allow ultra-low power consumption, reaching as low as 4.2 µA [17], at the expense of decimal precision in measurements. For these reasons—efficiency, low cost, and low power consumption—the BME280 was chosen for prototyping. Table 1 summarizes the measurement capabilities of the selected atmospheric sensor chips.

Table 1. Measurement capabilities of atmospheric sensor chips.

Chip	Monitored Variables	Manufacturer
SHT31	Temperature and Humidity	Sensirion
SHTC3	Temperature and Humidity	Sensirion
HTS221	Temperature and Humidity	STMicroelectronics
LPS22HB	Pressure and Temperature	STMicroelectronics
BMP280	Pressure and Temperature	Bosch
BME280	Temperature, Humidity, and Pressure	Bosch

Source: Prepared by the author based on [12–17].

Beyond atmospheric sensing, soil monitoring is indispensable. Integrated sensors from manufacturers like JXCT can measure up to seven variables, including temperature, moisture, pH, conductivity, and concentrations of potassium, nitrogen, and phosphorus in the soil [18]. While ideal for such applications, these sensors come at a high cost, ranging from R$200.00 to R$1000.00, exceeding the goal of developing a low-cost module. To maintain affordability while ensuring measurement of essential variables such as soil moisture and temperature, two sensors stand out as promising options.

The DS18B20, produced by MAXIM INTEGRATED, is a simple temperature sensor that uses a thermistor and communicates via the 1-Wire protocol, requiring only one wire for data transmission [19]. This feature poses a greater challenge when used with microcontrollers like the STM32, which demand precise timer and clock configuration due to the need for microsecond-level synchronization for accurate reading and writing. Despite this, the sensor stands out for its low cost and good accuracy. For soil moisture measurement, the capacitive ST0160 sensor from SunFounder appears as an economical and easy-to-integrate alternative. It operates by detecting changes in the soil's dielectric constant, which alters the capacitance between two conductive plates. This change generates an output voltage proportional to moisture, which can be read by the microcontroller to estimate soil moisture. However, these sensors may face corrosion issues in very wet or high-salinity soils.

After a brief overall review of the sensors and modules to be used in the project, one essential point remains. To be characterized as an embedded module, the capability for self-power supply is crucial. First, it is necessary to consider the existing technologies to calculate the maximum current consumption based on the information provided in manufacturers' datasheets. According to Table 2, it can be inferred that proper circuit operation requires at least 50 mA of current. To meet this demand, a polycrystalline silicon photovoltaic panel with 12 V and 5 W power rating will be used, providing an operating current of approximately 166 mA—more than sufficient to power the module.

Another fundamental aspect is energy storage, necessary to keep the system running during periods without sufficient sunlight on the photovoltaic cell. For example, a 4.2 V, 2500 mAh lithium polymer battery has the theoretical capacity to power the module for up to 50 h [20]. To ensure safe and efficient charging of this battery, a charge controller circuit is essential. The TP4057 is an IC specifically designed for this purpose, intended for linear charging of Li-Ion cells. It operates with a maximum supply voltage of 6.5 V and a charging voltage of 4.24 V. It also allows configuring the charging current between 100 mA and 500 mA via a resistor connected to the PROG pin and includes thermal regulation and charging status indicators [21].

Table 2. Comparison of Low-Power Atmospheric Sensor Chips.

Chip	Estimated Maximum Consumption	Chip
STM32F411CEU6	17.2 mA	STM32F411CEU6
nRF24L01 PA LNA	13.5 mA	nRF24L01 PA LNA
BME280	Less than 0.1 mA	BME280
DS18B20	1.5 mA	DS18B20
Soil Capacitive Moisture Sensor	20 mA	Soil Capacitive Moisture Sensor
Total:	47.2 mA	

Source: Prepared by the author based on [8,11,17,19].

The STM32, nRF24L01, and BME280 modules support a maximum voltage of 3.6 V and cannot be powered directly by the 12 V photovoltaic cell or the TP4057 charge controller. Therefore, a voltage regulator circuit is needed to step down from 12 V to 5 V to protect the charge controller. Among regulators, linear LDOs and switching Buck types stand out. LDOs are simple and inexpensive but dissipate power as heat, making them unsuitable for stepping down from 12 V to 5 V due to high thermal loss.

Switching Buck regulators are more efficient, using Pulse Width Modulation (PWM) to control voltage with minimal power dissipation. Their circuit involves a MOSFET, Schottky diode, inductor, and capacitor to smooth current and output voltage. The PWM duty cycle controls the output voltage, allowing high efficiency. For this project, the MP2331H Buck regulator was chosen, operating between 4.24 V and 24 V, supplying up to 2 A, and featuring internal undervoltage protections, ensuring safe and efficient power supply [22].

To power the circuits operating at 3.3 V, the linear regulator AMS1117-3.3 was chosen to step down the 5 V from the Buck converter. Due to the small voltage difference between input and output, power dissipation is low, estimated at about 85 mW for a maximum current of 50 mA and a voltage drop of 1.7 V. For monitoring the load cell voltage, the INA233 module from Texas Instruments is used, offering advanced measurement with a 16-bit Analog-to-Digital Converter (ADC), support for voltages up to 28 V, and current resolution up to 1.25 mA. It allows configurable sampling rates and digital calibration, with I^2C communication up to 1 MHz, enabling precise reading of electrical parameters [23].

3. Methodology

For the interconnection between components and integrated circuits, several protocols will be used. The nRF24L01 radio-frequency module, manufactured by Nordic Semiconductor (Trondheim, Norway), operates exclusively through the SPI protocol. The BME280 sensor, manufactured by Bosch Sensortec (Reutlingen, Alemanha), supports both SPI and I^2C, depending on its electrical configuration; however, SPI will be used to achieve higher data transfer rates. The external soil temperature and moisture sensors, DS18B20 and the Soil Moisture Sensor, communicate exclusively through the 1-Wire protocol. The INA233 uses the I^2C protocol for parameter reading and configuration.

The use of multiple communication protocols is mainly due to the system architecture and the limitations imposed by the chip manufacturers. As mentioned, the nRF24L01 is restricted to the SPI protocol, whereas the BME280 is not. The choice of using SPI and sharing the bus with the nRF24L01 was made exclusively to achieve higher data transfer rates.

Regarding the external sensors, the use of the 1-Wire protocol, besides being dictated by the sensor itself, also could not share the same protocols as the BME280, INA233, and the nRF24L01 transmitter module, since these sensors can and often must be located at much greater distances from the module than the BME280 and nRF24L01. Therefore, protocols such as SPI and I^2C would be problematic, as they are not designed for reliable data transfer

over distances greater than approximately 100 mm. Table 3 below compares and further describes each protocol used.

Table 3. Description and comparison between the protocols used.

Protocol	N° Wires	Distance	Speed
SPI	4	Short—100 mm max	10 Mbytes/s
I2C	2	Medium—about 500 mm	400 Kbytes/s in Fast Mode
1-Wire	1	Long—up to 100 m	15 Kbytes/s in Standard Mode

Source: Prepared by the author based on [24].

Regarding power supply, the photovoltaic cell output is connected directly to a Buck converter to step down the voltage from 12 V to 5 V, supplying both the TP4057 for charging the battery and the linear regulator AMS1117-3.3 V. The LDO converter output powers the sensitive circuit components and is also monitored by the INA233. Figure 1 shows the schematic of the main electrical connections between the modules.

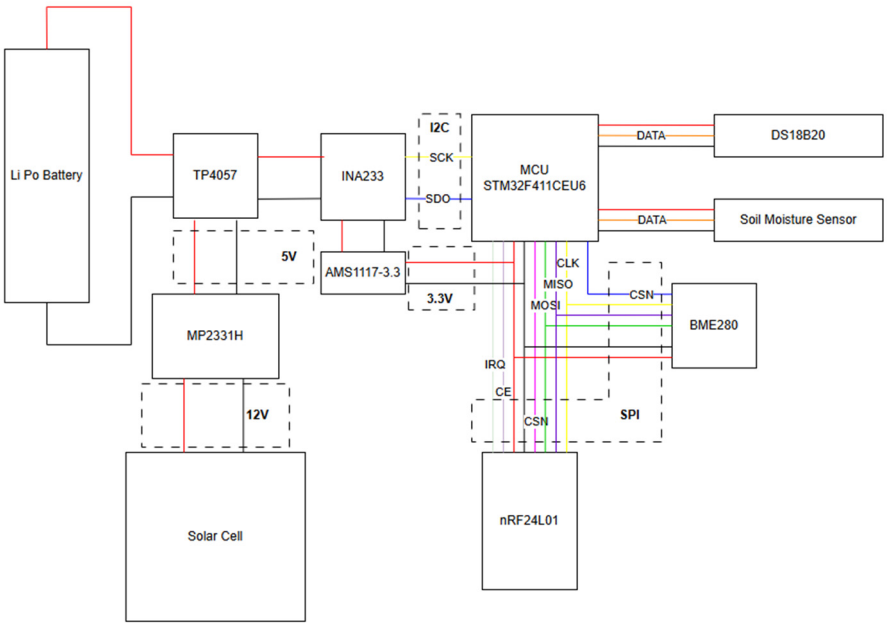


Figure 1. Schematic of the main electrical connections between the modules.

Following the electrical connection schematic shown in Figure 1, a bench prototype was assembled to evaluate the behavior of the sensors and validate the model. Figure 2 shows the following elements:

1. 12 V photovoltaic panel for general module power supply;
2. Buck converter configured for 12 V to 5 V, acting as the input voltage regulator;
3. Battery pack with TP4057 charging module;
4. LDO voltage regulator for stepping down from 5 V to 3.3 V;
5. STM32F411CEU (Black Pill) mounted on an acrylic plate for easier pin connections;
6. nRF2401L01+ PA LNA RF transmitter module;
7. BME280 combined sensor for humidity, pressure, and atmospheric temperature;
8. DS18B20 and Soil Moisture sensors mounted together.

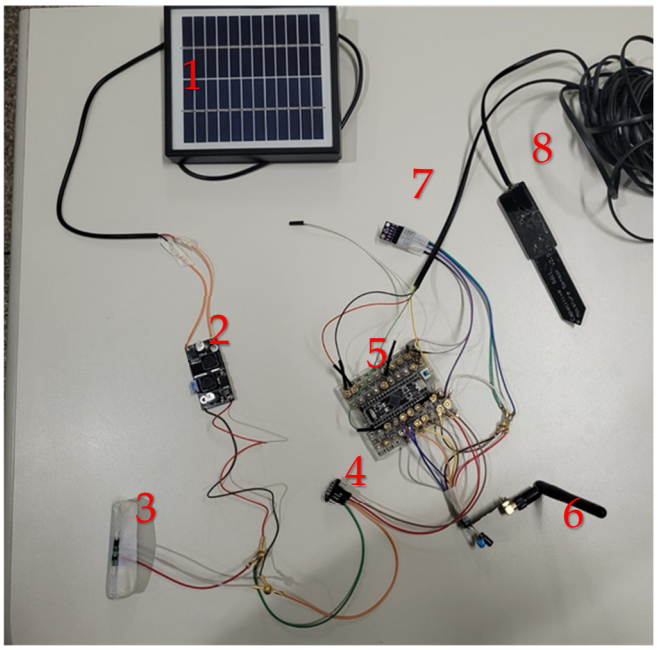


Figure 2. Prototype of Embedded Module for Agricultural Sensing.

It is possible to observe in Figure 3 the basic operational flow for data collection, processing, and transmission by the systems. On the left side, during module initialization, the components are configured in the following order: initialization and configuration of the nRF24L01, setting its registers with the transmission address in the data pipes used, transmission power, enabling dynamic payload length, and activating the Enhanced ShockBurst protocol. For the BME280, in order to reduce power consumption, the weather monitoring configuration recommended by the manufacturer was used. The IIR filter was disabled because the agricultural environment where the sensor operates does not present significant fluctuations in the measured parameters, making smoothing unnecessary. Regarding the DS18B20, its configuration does not require register settings; it only requires specifying the pin to which it is connected. Its communication and activation occur exclusively through precisely timed pulses, as defined in its datasheet. Similarly, the Soil Moisture Sensor does not require external configuration and outputs an analog voltage when powered on, which can be calibrated to represent the relative soil moisture.

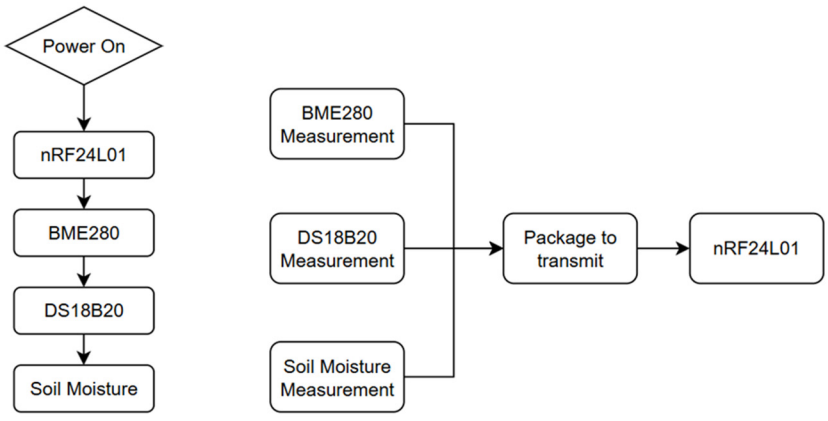


Figure 3. Flow of initialization, configuration, assembly, and transmission of the data packet collected in the module.

On the right side of Figure 3, the model for data collection, packet assembly, and transmission begins with sending a single-read command to the BME280, which, upon receiving it, exits low-power mode and performs measurements of humidity, pressure, and

atmospheric temperature. After that, the reading of the raw data registers recently collected by the BME280 is carried out, followed by their conversion into a structured format with temperature, humidity, and pressure values. For soil temperature, a read request pulse is sent to the DS18B20, which returns raw data for processing. Soil moisture measurement involves reading the analog voltage from the Soil Moisture Sensor (typically ranging from 300 mV to 6500 mV), converting it into a percentage value through the microcontroller's analog-to-digital converter (ADC). All processed data are then organized into a structure, converted into a byte array according to the format expected by the transmitter, and sent to the nRF24L01 for RF transmission.

4. Results and Discussion

As shown in Figure 2, the INA233 module is not present in the prototype assembly described in this work. This is because, as of the date of this article's preparation (9 August 2025), only three prototype assemblies had been built, and the integration of the INA233 was attempted only during the last one—unsuccessfully—due to the large number of required connections. However, in isolated module tests conducted for parameterization and driver evaluation, successful readings of load current and voltage were obtained.

Regarding the other measurement parameters, the module demonstrated consistent performance, responding in a stable and timely manner to environmental variations. The BME280, even when configured for low-power operation and with the IIR filter disabled, delivered satisfactory results, maintaining good accuracy in atmospheric pressure, temperature, and relative humidity measurements. Figure 4 below presents, in graphical form, the temperature values collected from the BME280 during isolated sensor tests.

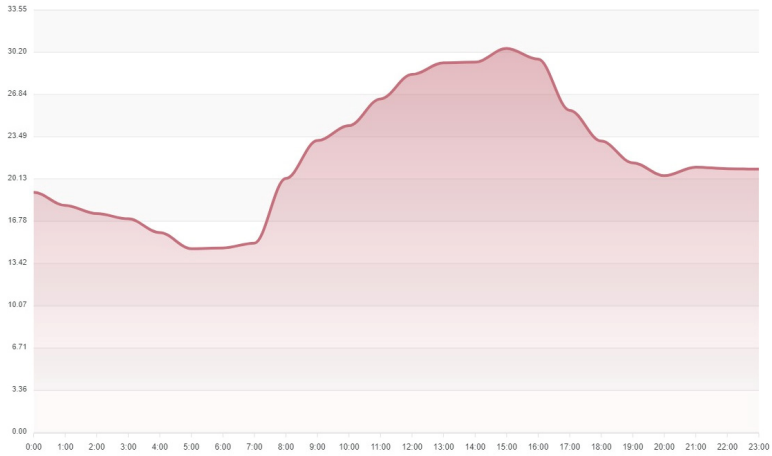


Figure 4. Atmospheric temperature data read from BME280 during bench test.

In addition, using a receiver for transmission testing, the module exhibited the expected behavior. When attempting to transmit without a receiver present, the chip did not receive transmission acknowledgment as required by the ESB (Enhanced Shock Burst) protocol configuration. This triggered an interrupt event via the IRQ pin, which the microcontroller interpreted—through reading the STATUS register—as a maximum retransmission condition.

With the protocol enabled, if a network error occurs that prevents the packet from being delivered, the module is notified and can act to resend the message, ensuring that every transmitted packet is correctly received. This gives the module a degree of autonomy while ensuring the reliability and integrity of the transmitted data.

In addition, Figure 5 below presents a graph of soil temperature data collected from the DS18B20 sensor. The measurements were carried out simultaneously with the BME280

data collection test. It can be observed that the DS18B20 indicated higher temperatures, which can be attributed to the greater thermal retention capacity of the soil.

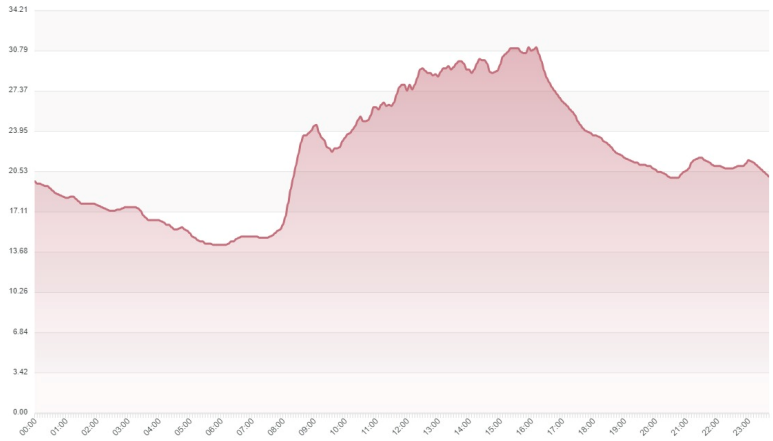


Figure 5. Soil temperature read data from DS18B20 during bench test.

The cost of the components used also remained within the established range of R$350, with a unit price of approximately R$157 before import taxes. The most expensive components were the photovoltaic panel, costing about R$37.42, and the transmitter module, priced at R$38.54. Table 4 shows the unit purchase cost of the components, sensors, and modules used.

Table 4. Unit purchase cost of the components, sensors, and modules used.

Module/Sensor	Cost (R$)
Soil Moisture	2.94
LDO 5 V 3.3 V	3.7
Solar Panel 12 V	37.42
Buck Converter	9.26
Charging controller	4.53
Transmitter module	38.54
Soil temperature sensor	26.62
Atmospheric sensor	19
Black Pill controller	15.6
Total Value:	157.61

Source: Data collected from AliExpress (2025).

Until now, no field tests of the module have been conducted due to difficulties in assembling a functional prototype from the component prototyping modules. Because of this limitation, it was not possible to proceed to subsequent stages such as receiver development and configuration of mesh network communication between transmitters. These aspects will be addressed in future work, including implementation, validation, and optimization of these functionalities.

5. Conclusions

The analysis of the results highlighted significant limitations in manually assembling the prototype from prototyping modules for practical use and scalability. The long fabrication time, risk of poor connections, performance variability between units, and the bulky size directly compromise the system's reliability, durability, and economic feasibility, making commercialization and even small-scale use unviable.

Given these limitations, the decision was made to develop a printed circuit board (PCB) integrating all components and sensors into a single board, Figure 6. This approach is

technically superior, enabling a more compact, robust, and standardized product, reducing production costs, minimizing assembly errors, and facilitating scalable replication.

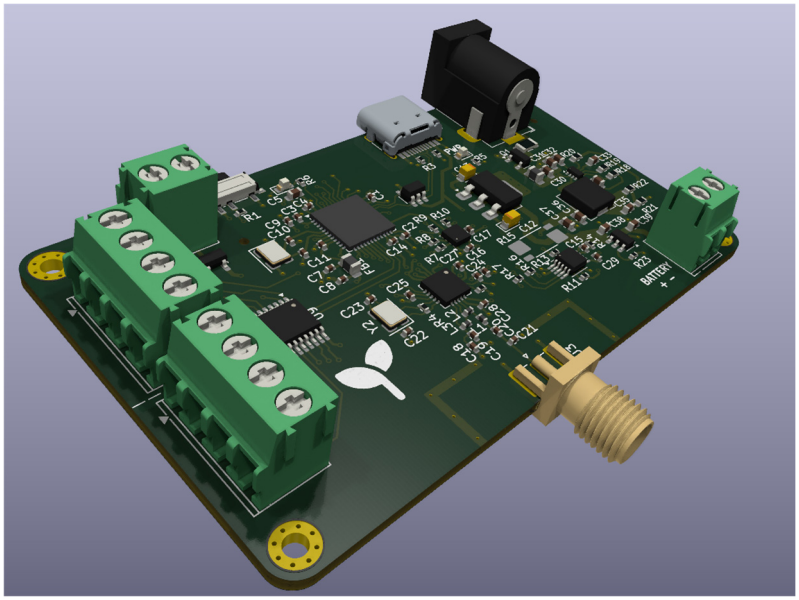


Figure 6. First look at the PCB design with all the modules and chips integrated.

Moreover, integrating components into a PCB will optimize electrical performance, reduce interference, and enhance mechanical strength, increasing reliability in field applications. This solution also allows better control over layout and thermal management—critical for continuous operation in rural environments.

In addition, it will greatly facilitate the application of protective agents such as resins and varnishes, ensuring proper operation even in chemically aggressive environments, such as planting regions. Due to the fixed dimensions of the PCB, it will also be possible to develop a custom 3D-printed enclosure, which, together with IP68 connectors for sensor interfacing and external power supply, will provide protection against splashes and environmental dust.

The next development phase will include finalizing the PCB design, manufacturing, laboratory testing, and field validation to verify system performance under real conditions. The outcomes will support future scientific publications and may foster partnerships for small- to medium-scale manufacturing, aiming to make the solution accessible to small and medium rural producers.

Author Contributions: Conceptualization, G.G. and W.N.L.; methodology, W.N.L.; software, G.G.; validation, investigation, data curation, writing—original draft preparation, writing—review and editing, supervision, project and administration, G.G., R.J.C., R.G.d.O.J. and R.d.O.A.T. All authors have read and agreed to the published version of the manuscript.

Funding: This research was funded by the Federal Institute of Paraná (IFPR), Brazil, through the Pro-Rectory of Extension, Research, Postgraduate Studies, and Innovation (PROEPPI) and the Agency for Innovation (AGIF), under the Unified Innovation Call (Edital nº 07/2024-PRADI/PIBITI).

Institutional Review Board Statement: Not applicable.

Informed Consent Statement: Not applicable.

Data Availability Statement: The data presented in this study are not publicly available due to confidentiality and ethical/proprietary restrictions imposed by the Research Group at IFPR. The data may, however, be made available upon reasonable request and justification to the corresponding author, Wenderson N. Lopes.

Acknowledgments: The authors thank AGIF and PROEPPI/IFPR for the financial support provided for this research. We are also grateful to IFPR–Campus Jacarezinho for the technical support and laboratory facilities, particularly the BitLabi[3]–Laboratory of Ideation, Innovation, and Analysis of Industrial Processes.

Conflicts of Interest: The authors declare no conflicts of interest.

References

1. Jornal da USP—Campus Ribeirão Preto. Mudanças Climáticas Afetam a Agricultura e Prejudicam a Produção de Alimentos. Jornal da USP: Ribeirão Preto, 5 March 2024. Available online: https://jornal.usp.br/campus-ribeirao-preto/mudancas-climaticas-afetam-a-agricultura-e-prejudicam-a-producao-de-alimentos (accessed on 27 July 2025).
2. Regis, M.S. Agricultura Digital: Adoção e Difusão no Brasil. Master's Thesis, Universidade de Brasília, Brasília, DF, Brazil, 2022. Available online: https://sigaa.unb.br/sigaa/public/programa/noticias_desc.jsf?lc=pt_BR&id=853&noticia=5180454 (accessed on 27 July 2025).
3. Jornal da USP—Atualidades. No País, Agricultura Familiar Representa 77% Dos Produtores e Apenas 23% da Renda Agrícola. *Jornal da USP, Atualidades*, 21 November 2024. Available online: https://jornal.usp.br/atualidades/no-pais-agricultura-familiar-representa-77-dos-produtores-e-apenas-23-da-renda-agricola (accessed on 28 July 2025).
4. Zhang, N.; Wang, M.; Wang, N. Precision agriculture—A worldwide overview. *Comput. Electron. Agric.* **2002**, *36*, 113–132. [CrossRef]
5. Redação Agro Estadão. O Que é e Como Funciona a Agricultura de Precisão? Agro Estadão, 2 May 2025. Available online: https://agro.estadao.com.br/summit-agro/o-que-e-e-como-funciona-a-agricultura-de-precisao (accessed on 27 July 2025).
6. Heble, S.; Kumar, A.; Prasad, K.V.V.D.; Samirana, S.; Rajalakshmi, P.; Desai, U.B. A Low Power IoT Network for Smart Agriculture. In Proceedings of the IEEE 4th World Forum on Internet of Things (WF-IoT), Singapore, 5–8 February 2018; Available online: https://people.iith.ac.in/raji/Cpapers/Smart%20Agriculture.pdf (accessed on 2 September 2025).
7. Math, R.M.; Dharwadkar, N.V. IoT based low-cost weather station and monitoring system for precision agriculture in India. In Proceedings of the 2nd International Conference on I-SMAC (IoT in Social, Mobile, Analytics and Cloud), Palladam, India, 30–31 August 2018; IEEE: New York, NY, USA, 2018; pp. 1–6. [CrossRef]
8. STMicroelectronics. STM32 32-Bit Arm Cortex MCUs, 2025. Available online: https://www.st.com/en/microcontrollers-microprocessors/stm32-32-bit-arm-cortex-mcus.html (accessed on 28 July 2025).
9. STMicroelectronics. STM32F411xC/E Advanced ARM®-Based 32-bit MCUs, Rev. 8, 2023. Available online: https://www.st.com/en/microcontrollers-microprocessors/stm32f411ce.html (accessed on 29 July 2025).
10. Chengdu Ebyte Electronic Technology Co., Ltd. E220 900T22D (E22 900T22D) LoRa User Manual/Datasheet, Latest Version. Available online: https://www.cdebyte.com/pdf-down.aspx?id=1136 (accessed on 29 July 2025).
11. Nordic Semiconductor ASA. nRF24L01 Single Chip 2.4GHz Transceiver: Product Specification, Rev. 2.0, July 2007. Available online: https://www.mouser.com/datasheet/2/297/nRF24L01_Product_Specification_v2_0-9199.pdf (accessed on 29 July 2025).
12. STMicroelectronics. HTS221: Capacitive Digital Sensor for Relative Humidity and Temperature, Datasheet, March 2023. Available online: https://www.st.com/resource/en/datasheet/hts221.pdf (accessed on 29 July 2025).
13. SENSIRION AG. Datasheet SHT3x-DIS: Humidity and Temperature Sensor, Version 7, December 2022. Available online: https://sensirion.com/media/documents/213E6A3B/63A5A569/Datasheet_SHT3x_DIS.pdf (accessed on 29 July 2025).
14. SENSIRION AG. Datasheet SHTC3: Humidity and Temperature Sensor IC, Version 4, December 2022. Available online: https://sensirion.com/media/documents/643F9C8E/63A5A436/Datasheet_SHTC3.pdf (accessed on 29 July 2025).
15. BOSCH SENSORTEC. BMP280: Digital Pressure Sensor, Version 1.26, October 2021. Available online: https://www.bosch-sensortec.com/media/boschsensortec/downloads/datasheets/bst-bmp280-ds001.pdf (accessed on 29 July 2025).
16. STMicroelectronics. LPS22HB: MEMS Nano Pressure Sensor—260–1260 hPa Absolute Digital Output Barometer, Datasheet, June 2017, Rev. 6. Available online: https://www.st.com/resource/en/datasheet/lps22hb.pdf (accessed on 29 July 2025).
17. Bosch Sensortec. BME280—Humidity Sensor, Rev. 1.24, February 2024. Available online: https://www.bosch-sensortec.com/products/environmental-sensors/humidity-sensors-bme280 (accessed on 31 July 2025).
18. JXCT. 7 in 1 Integrated Soil Sensor EC PH NPK Moisture Temperature Meter. Available online: https://www.jxct-iot.com/product/showproduct.php?id=197 (accessed on 31 July 2025).
19. Maxim Integrated. DS18B20 Programmable Resolution 1 Wire Digital Thermometer, Rev. 6, July 2019. Available online: https://www.mouser.com/catalog/specsheets/Soldered_101203.pdf (accessed on 31 July 2025).
20. Samsung SDI Co., Ltd. INR18650 25R Lithium Ion Rechargeable Cell: Product Specification, Spec No. INR18650 25R, Rev. 1.0, March 2014. Available online: https://www.powerstream.com/p/INR18650-25R-datasheet.pdf (accessed on 5 August 2025).
21. Shenzhen Tianyuan Semiconductor Co., Ltd. TP4057: 500 mA Linear Li Ion Battery Charger IC, 2024. Available online: https://mm.digikey.com/Volume0/opasdata/d220001/medias/docus/5010/TP4057.pdf (accessed on 5 August 2025).

22. Monolithic Power Systems Inc. MP2331HGTL Z (MP2331H) 24 V 2 A Synchronous Buck Converter: Product Datasheet, Rev. 1.0, October 2018. Available online: https://www.monolithicpower.com/en/documentview/productdocument/index/version/2/document_type/Datasheet/lang/en/sku/MP2331HGTL-Z/ (accessed on 5 August 2025).
23. AM Advanced Monolithic Systems. AMS1117: Voltage Regulators (LDO), Rev. 2017. Available online: https://mm.digikey.com/Volume0/opasdata/d220001/medias/docus/5011/AMS1117.pdf (accessed on 5 August 2025).
24. Embedded Security. Communication Protocols. Available online: https://embeddedsecurity.io/protocols (accessed on 24 August 2025).

Disclaimer/Publisher's Note: The statements, opinions and data contained in all publications are solely those of the individual author(s) and contributor(s) and not of MDPI and/or the editor(s). MDPI and/or the editor(s) disclaim responsibility for any injury to people or property resulting from any ideas, methods, instructions or products referred to in the content.